Space Charge Effect and Mirror Charge Effect in Photoemission Spectroscopy

X. J. Zhou[1,2], B. Wannberg[3], W. L. Yang[1,2], V. Brouet[1,2], Z. Sun[4], J. F. Douglas[4], D. Dessau[4], Z. Hussain[2] and Z.-X. Shen[1]

[1]*Dept. of Physics, Applied Physics and Stanford Synchrotron Radiation Laboratory, Stanford University, Stanford, CA 94305*

[2]*Advanced Light Source, Lawrence Berkeley National Lab, Berkeley, CA 94720*

[3] *Gammadata Scienta AB, P.O. Box 15120, SE-750 15 Uppsala, Sweden*

[4]*Department of Physics, University of Colorado, Boulder, Colorado 80309-0390*

(Dated: August 2, 2004)

Abstract

We report the observation and systematic investigation of the space charge effect and mirror charge effect in photoemission spectroscopy. When pulsed light is incident on a sample, the photoemitted electrons experience energy redistribution after escaping from the surface because of the Coulomb interaction between them (space charge effect) and between photoemitted electrons and the distribution of mirror charges in the sample (mirror charge effect). These combined Coulomb interaction effects give rise to an energy shift and a broadening which can be on the order of 10 meV for a typical third-generation synchrotron light source. This value is comparable to many fundamental physical parameters actively studied by photoemission spectroscopy and should be taken seriously in interpreting photoemission data and in designing next generation experiments.

Key words: Space charge, mirror charge, photoemission, Fermi level shift, Fermi level broadening.

I. INTRODUCTION

Photoemission spectroscopy measures the energy distribution of photo-emitted electrons when materials are irradiated with light [1, 2](Fig. 1). It is widely used in solid state physics and chemistry for investigating the electronic structure of surface, interface and bulk materials[1, 2]. Recently it has become a prime choice of technique in studying strongly correlated electron systems[3, 4], such as high temperature superconductors[5]. The availability of synchrotron light sources and lasers, combined with the latest advancement of electron energy analyzer, has made a dramatic improvement on the energy resolution of photoemission technique in the last decade; an energy resolution of $\sim$ 5meV or better can now be routinely obtained. These achievements have made it possible to probe intrinsic properties of materials and many-body effects[5]. For example, measurements of the superconducting gap on the order of 1 meV, as in conventional superconductors[6] and in some high temperature superconductors[7], have been demonstrated.

On the other hand, the utilization of pulsed light sources, such as synchrotron light or pulsed lasers, has also brought about concerns of the space charge effect[8]. When a large number of electrons are generated from a short pulsed source and leave the sample surface, the electrons will first experience a rapid spatial distribution depending on their kinetic energy. Then, because of the Coulomb interaction, the fast electrons tend to be pushed by the electrons behind them while the slow electrons tend to be retarded by those fast electrons. This energy redistribution will distort the intrinsic information contained in the initial photoelectrons by giving rise to two kinds of effects. One is a general broadening of the energy distribution, due to both acceleration and retardation of electrons in their encounters. The other is a systematic shift in the energy. The space charge broadening of the energy distribution has been known for a long time as a limiting factor in electron monochromators and other electron beam devices[9], but it has not been considered in photoemission until very recently[8]. The main concern there was whether such an effect will set an ultimate limit on further improving the energy resolution of the photoemission technique[8].

Here we report the first experimental observation of the space charge effect in photoemission. In addition, by combining experimental measurement with numerical simulations, we show that the mirror charges (also known as image charges in the literature) in the sample also play an important role in the energy shift and broadening. The combined effect of

these Coulomb interactions gives an energy shift and broadening on the order of 10 meV for a typical third-generation synchrotron light source, which is already comparable or larger than the energy resolution set by the light source and the electron analyzer. The value is also comparable to the many-body effect actively pursued by modern photoemission spectroscopy. These effects, therefore, should be taken seriously in interpreting experimental data and in designing next generation experiments.

II. EXPERIMENT

The experiment was carried out on beamline 10.0.1 at the Advanced Light Source. This is a third-generation synchrotron source which generates pulsed light with a frequency of 500 MHz and a duration of ∼60 ps. The beamline can generate linearly-polarized bright ultraviolet light with a photon flux on the order of 10^{12} photons/second with a resolving power E/ΔE of 10,000 (E is the photon energy and ΔE the beamline energy resolution). The endstation is equipped with a high resolution Scienta 2002 analyzer. The analyzer, together with the chamber, is rotatable with respect to the beam while the sample position is fixed. The measurement geometry is illustrated in the upright inset of Fig. 1. There are two angles to define the direction of electrons entering the analyzer with respect to the sample normal: tilt angle ϕ and analyzer rotation angle α. We measured the sample current to quantitatively measure the number of electrons escaping from the sample which is proportional to the photon flux. With the pulse frequency of 500MHz at the ALS, 1 nA of the sample current corresponds to 12.5 electrons per pulse.

Fig. 2a shows a typical photoemission spectrum of polycrystalline gold taken with a photon energy of 35 eV. It consists of a Fermi edge drop (E_F) near ∼30 eV, valence band between 20∼30eV and a secondary electron tail extending to lower kinetic energy arising from the inelastic scattering. We chose to measure on gold because the sharp Fermi edge at low temperature (∼20 K for all the measurements in the paper) gives a good measure of both the energy position and width (Fig. 2b). The Fermi edge is fitted by the Fermi-Dirac function, f(E)=$1/(exp(\frac{E-E_F}{k_BT})+1)$, at zero temperature convoluted with a Gaussian with a Full-Width-at-Half-Maximum (FWHM) Γ. This width Γ includes all the contributions from thermal broadening, analyzer resolution, beamline resolution and others.

In photoemission experiments, it is a routine procedure to use Fermi level of a metal (such

as gold) as the energy referencing point for the sample under study because the Fermi levels are expected to line up with each other when the metal and the sample are in good electrical contact. The Fermi level of the metal is also expected to be dependent only on the photon energy and not on other experimental conditions, such as sample temperature, photon flux etc. It was therefore quite surprising when we first found out that the gold Fermi edge shifts position with incident photon intensity (Fig. 2b). A systematic measurement reveals that, under some measurement geometries, the Fermi level varies linearly with the sample current and the shift can be as high as ∼20meV within the photon flux range measured (Fig. 3a). Note that the Fermi level energy gets higher with increasing photon flux. This rules out the possibility of sample charging that usually occurs due to poor electrical grounding of the sample. In that case, the Fermi level energy would be pushed downward with increasing photon flux. We can also rule out the possibility of the local sample heating due to high photon flux because temperature only affects the Fermi edge broadening but will not change the Fermi level position. As we estimated, for a photon flux of $\sim 10^{13}$ photons/second at a photon energy of 35 eV, the corresponding power is ∼0.056 mW. The temperature increase with such a small power, spread over an area of 1 mm^2, is negligible so it also has little effect on the thermal broadening of the Fermi edge.

The first thing to check is whether this Fermi level shift with photon flux is due to instrumental problems, which can be from either the beamline or the electron analyzer. Regarding the beamline, the photon flux is usually varied by adjusting the size of the beamline slits. This will change the beamline energy resolution correspondingly but may potentially also cause energy position change. To check whether this is the case, we put a photon blocker in the beamline (Fig. 1) so that it can attenuate the photon flux while keeping the photon energy and resolution intact. Using the photon blocker, we observed a similar variation of the Fermi level with photon flux (Fig. 3a), thus ruling out the possibility of beamline problems. We also put an electron blocker (Fig. 1) to vary the number of electrons collected by the analyzer. When the photon flux on the sample is fixed, the Fermi edge shows little change with the number of electrons entering the analyzer (Fig. 3b). This indicates that the energy shift we have observed is not due to problems of the electron analyzer either. Therefore, the observed energy shift must be associated with the photoemission process itself.

In addition to the energy position shift, there is also an energy broadening associated with increasing photon flux. To observe such an effect, we have to compromise the beamline

energy resolution in the way that it has a relatively high photon flux to induce an obvious broadening effect, and a relatively high energy resolution (∼10meV) in order to resolve the additional broadening from all other contributions. The measurement is made possible by taking the advantage of the photon blocker to fix the contribution from the beamline. The total width increases with increasing photon flux (inset of Fig. 4). Taking the width at the lowest photon flux as arising from all the other contributions including the beamline, the analyzer and sample temperature broadening, the photon-induced energy broadening can be extracted after deconvolution. As seen in Fig. 4, it varies with the photon flux with a magnitude comparable to but slightly larger than the energy shift.

We have found that the Fermi edge shift and broadening are sensitive to the spot size of the beam on the sample (Fig. 5). Here the spot size is changed by varying the vertical focus of the beamline; the horizontal beamsize is fixed. It is measured using the transmission mode of the analyzer, calibrated by using samples with known size. As seen from Fig. 5a, as the spot size increases, the energy shift gets less sensitive to the change of photon flux, as also seen from the slope change as a function of the spot size (Fig. 6). For comparison, Fig. 6 also includes the simulated data over a large range of spot sizes. Although the data of energy broadening (Fig. 5b) is scattered as a result of deconvolution from a relatively large background value, the trend is clear that the broadening gets smaller with increasing spot size. Again, for a given beam size, the magnitude of the energy broadening is comparable to but slightly larger than the corresponding energy shift.

The Fermi edge shift and broadening are also sensitive to the electron emission angle. We set the gold sample at different tilt angles and measured the Fermi level position and width as a function of the analyzer angle under various photon flux. As seen in Fig. 7, the Fermi level position exhibits a strong variation with the analyzer angle, particularly at high photon flux. The Fermi level is higher near smaller analyzer angle and decreases with increasing analyzer angle. When the analyzer angle is close to 90 degrees all the curves with different sample tilt angle and with different sample current tend to approach to a similar position within the experimental error. The overall measured Fermi level width basically follows the trend of the energy shift: it becomes smaller with increasing analyzer angle. We also notice that the curves are not symmetrical with respect to the zero analyzer angle. Since the surface of the polycrystalline gold we used is not perfectly flat, one possible reason is that the exact angle may be slightly off from the nominal value. Another possibility is

the presence of a small systematic error. As indicated from Fig. 7, when the sample current is small (23 nA), one can still observe Fermi level shift with the analyzer angle which may be due to a systematic error associated with the experimental setup.

To gain more insight on the angle dependence, we also measured the energy shift and broadening as a function of the sample current at different analyzer angles (Figs. 8a and b). It is interesting to note that, while for small analyzer angles, the energy shift is proportional to the sample current, as we have seen before, it deviates significantly from the straight line for large angles. In this case, the energy shift exhibits linear relation only at high sample current. When the sample current gets smaller, it goes through a minimum, and then gets larger again even with further decreasing of the sample current. One may expect that at zero sample current the energy shift approach zero so that all curves should converge at the zero sample current, as indeed shown by the data in Fig. 8 (the small Fermi level scattering at zero sample current may be due to the systematic error as discussed before). This implies that, for large analyzer angles, the energy shift can be even negative at some sample current.

Fitting the high sample current part of the curves in Figs. 8a and b with a straight line, we extracted their slopes and plotted them in Fig. 8c for two sample tilt angles. The shape of the curves is similar to that in Fig. 7. The high sample current part overlaps with each other. When extrapolated to 90 degrees the Fermi level shift is approaching zero which is also consistent with the converging of the Fermi level at high analyzer angle as seen in Fig. 7.

To further investigate the origin of the angle-dependent energy shift and broadening, we measured the gold valence band at different analyzer angles (Fig. 9). The intensity of these spectra are normalized to the photon flux so they are comparable with each other. The shape of the valence band shows no obvious change with the analyzer angle, but their relative intensity changes dramatically. For a quantitative comparison, we integrated the spectral weight over a large energy range (5$\sim$35 eV) and the result is shown in the inset of Fig. 9. Integration over a smaller energy window such as 25$\sim$35 gives essentially the same shape. We have found that the angular variation of the relative valence band intensity and the Fermi level shift is identical (inset of Fig. 9). This indicates that the angle dependence of the Fermi level is directly related to the angle-dependence of the number of photo-emitted electrons.

III. NUMERICAL SIMULATION OF SPACE CHARGE EFFECT AND MIRROR CHARGE EFFECT

It is expected that the space charge effect depends on a number of parameters[8]: (1). the number of electrons per pulse; (2). the pulse length; (3). the size and shape of the excitation area; and (4). the energy distribution of the electrons. We have performed numerical simulations using the Monte Carlo-based technique developed earlier[8] in order to quantitatively examine our results. This serves first to check whether the observed energy shift and broadening can be entirely attributed to the space charge effect. It then helps to understand the microscopic processes associated with it, such as the time scale of the process. Moreover, it can be extended to investigate situations that are difficult or not accessible for the experiments, such as the effect of the electron energy distribution, the effect of the pulse length, and the case of a continuous source, as we will discuss below.

In the simulation, a specified number of electrons (1-100000) (denoted as interaction electrons hereafter) are started at random positions within the specified source area, at random times during the pulse, and with random energies with some specified distribution. Because the acceptance angle of the electron energy analyzer is small, the electrons for which the energy spread and broadening are to be calculated (denoted as test electrons hereafter) are started in the forward direction with a specified initial energy but with a random distribution in start position and time. This condition corresponds to the measurement geometry of the analyzer angle α=0 and the sample tilt angle ϕ=0. Each test electron is assumed to feel the Coulomb force from all interaction electrons within some cut-off distance. The interaction electrons are assumed to move in straight lines defined by their initial conditions, i.e. all mutual interactions between them are neglected. This is legitimate because their position changes are extremely small and random. The energy evolution of a single test electron is followed until all interaction electrons have vanished outside the cut-off distance. Then, the process is repeated with a new set of interaction electrons and one new test electron. This procedure is repeated a few thousand times, after which the energy distribution of the test electrons is calculated. For the accuracy of the integration to be of the same order of magnitude as the statistical uncertainty, the cut-off distance has to be at least 1 mm, and for most calculations it was chosen to be 2 mm. The energy distribution can usually be well fitted by a Gaussian, although the number of electrons which experience very large shifts is

significantly larger than for the Gaussian distribution. Such extreme outliers are neglected when calculating the width of the distribution.

The electrons in the pulse will experience Coulomb interaction from all the other electrons at different energies, including the large number of low-energy secondary electrons (Fig. 2a). To evaluate the effect of the electron energy distribution on the electrons at the Fermi level , we divided the energy range below E_F into a number of regions, and calculated the contribution from each individual region. The simulated energy shift and broadening from the direct space charge effect are plotted in Figs. 10a and 10b, respectively. The energy shift displays a strictly linear relation with the number of electrons in a pulse and the slope as a function of test electron kinetic energy is plotted in Fig. 11. On the other hand, the energy broadening exhibits a nearly linear relation only at large number of electrons; at small number of electrons it shows a bend. Clearly all electrons contribute to the Fermi level energy shift and broadening but they contribute differently: the high-energy electrons contribute more than the low-energy ones (Fig. 11).

In fact, an electron at a distance z in front of a conducting metal surface will also experience an attractive force $F(z)=-e^2/(2z)^2$, identical to that produced by a positive (mirror image) charge at a distance z inside the metal[10]. The basic assumption behind the mirror charge concept is that the charges on the sample surface redistribute themselves in such a way that the surface is always an equipotential surface. Whether this assumption is correct on the time scale considered here may be dependent, e.g., on the conductivity of the sample. In this case, each interaction electron is accompanied by a mirror charge in the sample (inset of Fig. 12a), which also interacts with the test electron. The interaction of the test electron with its own mirror charge is not included here because it is always present. In the earlier simulation[8], the mirror charges could be neglected when only considering the broadening caused by interaction electrons with energies close to that of the test electron. For the case when the test electron has higher energy than all interaction electrons, this is no longer true, in particular when the energy shifts are also considered.

Fig. 12a and 12b show simulated energy shift and broadening for different energy ranges by incorporating both the space and mirror charge effects. The energy shift retains a linear variation with the number of test electrons per pulse and the slope is plotted in Fig. 11. The contribution from the mirror charge alone can be easily extracted. Apparently the mirror charge gives rise to a negative energy shift with increasing number of electrons per

pulse. This helps in compensating the positive energy shift from the space charge effect. The combined effect on the energy broadening is more complicated. For the highest energy range of the interaction electrons (25 - 30 eV), the combined broadening (Fig. 12b) is larger than that from the space charge effect alone (Fig. 10b). But for the lower energy range of the interaction electrons, it is smaller than that from the space charge effect.

We have found that the energy shift and broadening occur at very different time scales. As seen from Fig. 13, the energy shift evolves gradually within the first nanosecond. The energy broadening, on the other hand, has already reached its equilibrium value at 100 ps, followed by random fluctuations. This is because the energy shift takes place only after the electrons have spatially sorted themselves according to their energy; after that the forces are all acting in the same direction. We also note that initially each interaction electron and its mirror charge form a very short dipole, from which the field decreases rapidly with distance. The broadening, on the other hand, is much more of a nearest-neighbor effect, which is strongest when the pulse is dense. Detailed study of the energy evolution for individual electrons shows that the random part of the energy change is often dominated by one single event, i.e., a close encounter with another electron. Since the energy shift continues to grow over a time that is comparable to the interval between pulses, we have also checked whether it can be affected by remaining slow electrons from the previous pulse: we have found that this contribution is completely negligible.

Since a time-continuous light source, such as discharge lamps, is widely used as a lab source for photoemission, it is important to check whether similar effects still exist in that case. For a continuous light source, because there will be no spatial redistribution of the electrons according to their energy, one might expect the contribution to the energy shift from the space charge to be close to zero, while the mirror charge will give a negative shift. The broadening can be expected to be of the same order of magnitude as that from a pulsed source with the same number of electrons per unit time. To simulate a continuous source, we first start with a pulsed source, varying the pulse length while keeping the number of electrons per unit time constant, and try to extrapolate to infinite length to approximate a continuous source. We have considered a typical case of Helium I radiation (photon energy 21.12eV) on polycrystalline gold, and varied the sample current during the pulse from 0.15 to 50 electrons/ps. Fig. 14 shows the energy shift and broadening for different sample currents as a function of the pulse length. When scaled by the sample current, all energy shift curves

overlap with each other because the shift is proportional to the current for all pulse lengths (Fig. 14a). The energy shift shows non-monotonic dependence with the pulse length, owing to the competition between the direct space charges and mirror charges. When the pulse length is short, the space charge dominates which gives positive energy shift. When the pulse length is long enough, the effect from mirror charges dominates which leads to a negative energy shift. Eventually it asymptotically reaches a value that can be taken for a continuous source. The shift is -0.7meV for 1.5×10^{12} electrons/second and can get significant when the photon flux is larger. The energy broadening (Fig. 14b), on the other hand, does not scale with the sample current, particularly at longer pulse length. It also exhibits a non-monotonic variation with the pulse length, reaching a maximum around 10^4 ps and then decreases with further increasing of the pulse length. If we assume an asymptotic behavior following the drop, the broadening for the continuous source is close to 1 meV for a sample current of 1.5×10^{12} electrons/second.

IV. COMPARISON BETWEEN THE EXPERIMENT AND THE NUMERICAL SIMULATION AND DISCUSSIONS

As we have seen from both the experimental measurements and the simulation, the energy shift and broadening depend on many parameters, such as the number of electrons per pulse, the pulse length, the spot size on the sample, the emission angle of electrons and the photon energy used. Moreover, it is material-specific. This is first because it depends on the shape of the valence band, i.e, the energy distribution of photoelectrons. Seocnd, for metals and insulators, the effect of mirror charge may vary significantly. With so many factors coming into play simultaneously, it is hard to exhaust all the possibilities and a proper approach to take is to measure or simulate on an individual basis.

As shown in Figs. 4 and 5, the measured energy shift is proportional to the sample current and the broadening is nearly linear at high sample current and shows a bend at lower sample current. Qualitatively speaking, both observations are consistent with the simulated results from either the space charge effect (Fig. 10) or combined space and mirror charge effects (Fig. 12). After obtaining the contribution for each individual energy range from the space charge effect (Fig. 10), we calculated the overall energy shift from the measured valence band (Fig. 2a) as a weighted sum of the contributions from the different energy ranges. We

also used a model where the energy distribution is approximated by a rectangular shape corresponding to the valence band and a triangular distribution of the secondary electrons; the obtained results are similar. It was found that the value for the energy shift obtained from the space charge effect alone is much higher than that measured from experiment. For example, for the spot size of 0.43mm×0.42mm, the calculated energy shift is 0.175 meV/nA, much higher than the measured 0.055 meV/nA. The large discrepancy indicates that the space charge effect alone can not account for the observed energy shift. This prompted us in identifying the mirror charge effect that should be present for metals such as gold. After considering both effects(Fig. 12), the calculated energy shift becomes quantitatively consistent with the experiment, as seen in Fig. 6 even for different spot sizes. Considering that there are no adjustable parameters in the simulation, this level of agreement is striking. This indicates that we have captured the main contributors to the energy shift effect. The quantitative comparison between the measurement and the simulation has made us able to identify the mirror charge effect that was not included before[8].

For the area dependence (Fig. 6), we note that the size of the spot on the sample relative to the distance an electron travels during the pulse is important. Depending on the relative ratio, the space charge effect may exhibit different dependence on the spot size. If the light spot is much larger than the electron travelling distance (for 30 eV electron, the travelling distance is ∼0.2 mm within 60 ps), the shape of electron spatial distribution is basically flat. The space charge effect is expected to be proportional to the number of electrons/area. When the spot size gets smaller, one will get increasingly important edge effects, because electrons that move outside the spot will not be compensated by electrons coming from the outside. In the limit where the spot is very small, the spatial distribution of electrons is a half-sphere. The average distance between electrons will be defined by their time interval rather than by the distance between the points where they started. So in that case, the effect may become independent of the spot size.

On the other hand, there are cases where the simulation deviates from measurements. We found that the measured broadening is larger than the values calculated from the simulation. As shown in Fig. 6, from the simulation, the broadening is smaller than the shift whereas from the measurement (Fig. 4 and 5), the broadening is comparable or slightly larger than the shift. The reason for this discrepancy is not clear yet and probably more sophisticated simulations are needed to address the discrepancy. We note the broadening can be larger

than the shift when the energy of the interaction electrons is close to that of the test electron (energy range 25∼30 eV in Fig. 12b) which is probably due to the longer average interaction times. However, in the case of gold, because the fraction of electrons in the range close to the Fermi edge is very small (Fig. 2a), this contribution is small to the overall broadening. The angular dependence of the energy shift (Fig. 7) can be well attributed to angle-dependent number of electrons at different emission angles (Fig. 9) which is probably associated with the linear polarization of the synchrotron light. However, to understand the negative energy shift for high analyzer angles at lower sample current, more simulation is also needed.

V. IMPLICATIONS OF SPACE CHARGE EFFECT

The observation of space and mirror charge effects has important implications in photoemission experiments as well as the future development of the technique. These findings first ask for particular caution in interpreting photoemission data. One immediate issue is the electron energy referencing in photoemission spectroscopy. In photoemission community it is a routine procedure to use the Fermi level of a metal as a reference. This is usually realized by measuring the Fermi level from a metal (such as gold) which is electrically connected to the sample under measurement. It is true that the intrinsic Fermi level of the sample is lined up with that of the metal, but the measured Fermi level has an offset from the space and mirror charge effects. This offset can be different between the sample and the metal because it is not only material-specific, but also depends on many other factors. When the effect on the energy shift is strong, using the Fermi level from a metal as a reference becomes unreliable.

Another related issue is the Fermi level instability during measurement. Because the photon flux usually changes with time for many synchrotron light sources due to the finite life-time of electrons in the storage ring, the Fermi level is always changing with time during measurements. As we have shown before, this can give rise to an Fermi level uncertainty on the order of 10 meV for a typical experimental setting using a third-generation synchrotron light source. This is comparable or larger than many energy scales which are actively pursued in many-body problems in the condensed matter physics[3, 4]. Measurement with an energy precision of 1 meV is necessary, for example, when the superconducting gap in some conventional metals as well as in some high temperature superconductors is on the

order of 1 meV[6, 7]. In this case, an uncertainty or shift on the order of 10 meV definitely poses a big problem.

To resolve the Fermi level referencing problem, one can always minimize the space charge effect by reducing the photon flux, or increasing the spot size. Apparently this is not desirable, particularly when a high photon flux is necessary to take data with a good statistics and a high efficiency. Given that the Fermi level referencing to a metal is no longer reliable, one may use an internal reference from the sample under measurement. This internal reference can be obtained from *priori* knowledge or measurements with negligible space charge effect. For example, in high temperature cuprate materials, the (0,0) to (π,π) nodal direction can be used as an internal reference to locate the Fermi level because it has been shown that the superconducting gap and pseudogap approaches zero along this direction except for slightly doped samples[5]. As for the Fermi level instability with time, since the energy shift exhibits a linear relation with the photon flux, it is possible to make corrections by recording the sample current or photon flux. Ideally, this problem can be minimized if the synchrotron light source is operated at a constant or quasi-constant photon flux ("Top-off") mode.

In addition to the Fermi level uncertainty, the energy broadening is another serious issue facing the photoemission technique. Since most physical properties of materials are dictated by electronic excitations within an energy range of $\sim k_B T$ near the Fermi level (k_B is the Boltzman constant and T a temperature), to probe the intrinsic electronic properties, the energy resolution has to be comparable or better than $k_B T$, which is 0.8 meV for 10 K. Therefore, there is a strong scientific impetus to improve the photoemission technique to even higher energy resolution (sub-meV), accompanied by high photon flux and small beam size. The space and mirror charge effects should be taken into account seriously in the future development of new light sources and electron energy analyzers. The high photon flux and small spot size will enhance the space and mirror charge effects; the resultant energy broadening can be well beyond the resolution from the electron analyzer and the light source.

With the increasing demand of high energy resolution, it is important to investigate how to alleviate or remove the space charge effect. For example, it is interesting to study whether applying a bias voltage between the sample and the electron detector will affect the space charge effect. On the other hand, in addition to putting more effort on improving the performance of the light sources, it is very important to put emphasis on enhancing the

capabilities of the electron energy analyzer. One aspect is to further increase the sensitivity of electron detection by using new electron detection schemes. The other aspect is to keep improving the analyzer throughput. Note that even for the state-of-the-art display electron analyzer, using angle-resolved mode, only less than 1% of electrons are collected during measurements while all the rest of electrons emitted over 2π solid angle from the sample surface are wasted. A new scheme needs to be explored on how to record large solid angle at the same time when maintaining high energy resolution. It is apparent that much work needs to be done and we hope our identification of the Coulomb effects can stimulate more work along this direction.

---

[1] S. Huefner, Photoemission Spectroscopy: Principles and Applications (Springer-Verlag, Berlin, 1995).

[2] Angle-Resolved Photoemission: Theory and Current Applications, edited by S. D. Kevan, (Elsevier, The Netherlans, 1992).

[3] Special issue of Science **288**, No. 5465, (2000).

[4] Special issue of J. Electron Spectroscopy and Related Phenomena, **117-118** 1(2001).

[5] A. Damascelli, Z. Hussain and Z.-X. Shen, Rev. Modern Phys. **75**, 473(2003).

[6] A. Chainani et al., Phys. Rev. Lett. **85**, 1966(2001).

[7] N. P. Armitage et al., Phys. Rev. Lett. **86**, 1126(2001); T. Sato et al., Science **291**, 1517(2001).

[8] B. Wannberg, P. Baltzer and S. Shin, preprint (2000).

[9] H. Boersch, Z. Physik **139**, 115 (1954).

[10] U. Hofer et al., Science **277**, 1480 (1997); P. M. Echenique and J. B. Pendry, Progress in Surf. Sci. **32**, 111 (1989).

[11] We thank A. Fujimori, J. Bozek and S. Sodergren for stimulating discussions. The experiment was performed at the ALS of LBNL, which is operated by the DOE's Office of BES, Division of Material Science, with contract DE-FG03-01ER45929-A001. The division also provided support for the work at SSRL with contract DE-FG03-01ER45929-A001. The work at Stanford was supported by NSF grant DMR-0304981 and ONR grant N00014-98-1-0195-P0007, and the work at Colorado was supported by NSF grant DMR 0402814 and DOE grant DE-FG02-03ER46066.

FIG. 1: Schematic of photoemission setup. A pulsed light is incident on the sample, kicking out electrons, and the electrons are collected by the electron energy analyzer. The photon blocker is used to change photon flux while keeping the beamline intact. The electron blocker is used to change the number of electrons collected by the analyzer. The sample current recorded by a picoammeter measures the number of electrons out of the sample which is proportional to the photon flux. In the upright inset shows the measurement geometry of the light, the sample and the analyzer. The synchrotron light is along the X axis, with its electrical field $\vec{E}$ in the XY horizontal plane and parallel to Y axis. The sample normal is in the XZ plane and its angle with respect to the Z axis is referred to as ϕ. The analyzer is rotatable and the lens axis is in the YZ plane. The angle of the lens axis with respect to the Z axis is referred to as α.

FIG. 2: Photoemission spectra of a polycrystalline gold measured at a photon energy of 34 eV and a temperature of 20K. (a). Large energy range spectrum showing a Fermi cutoff at 29.38eV, the valence band between 20 and 30 eV, and lower energy part arising from secondary electrons. (b). Au Fermi level measured at different photon flux, as indicated by different sample current. The open circles are experimental data which are fitted by Fermi-Dirac functions (lines).

FIG. 3: Fermi level shift in photoemission process. The sample tilt angle ϕ is 45 degrees and the analyzer angle α is 0. (a). Fermi level shift with the sample current varied by either varying the beamline slits (solid circle) or by using the photon blocker (open square). (b). Fermi edge shift as a function of the number of electrons entering the analyzer varied by either changing the photon flux by using the photon blocker(open square) or keeping the photon flux constant but using the electron blocker (solid circle).

FIG. 4: Fermi edge broadening (solid square) and the Fermi edge shift (open circle) as a function of sample current. The sample tilt angle ϕ is 45 degrees and the analyzer angle α is 0. The beam spot size is $\sim 0.43\times0.30$ mm^2. The photon flux corresponding to 150 nA sample current is $\sim5\times10^{13}$ photons/second. The inset shows the measured overall Fermi edge width as a function of the sample current, which includes all contributions including the beamline, the analyzer and the temperature broadening. The net broadening resulting from pulsed photons is obtained by deconvolution of the measured data, taking the width at low photon flux as from all the other contributions.

FIG. 5: (a). Effect of beam spot size on the energy shift. The energy shift for each spot size (FWHM) shows a nearly linear dependence on the sample current and is fitted with a straight line (solid lines). The sample tilt angle ϕ is 45 degrees and the analyzer angle α is 0. (b). Effect of beam size on the energy broadening. The broadening at high sample current can be approximated as a straight line; the solid lines also act as a guide to the eye.

FIG. 6: Effect of beam spot size on the energy shift and broadening. The measured energy shift (solid square) is obtained from the slope by fitting the curves in Fig. 5a with linear lines. The simulated energy shift (open square) and broadening (open circle), are calculated by considering both the space and mirror charge effects and the overall gold valence band as shown in Fig. 2a.

FIG. 7: The energy shift (upper panel) and broadening (lower panel) as a function of the analyzer angle α for different sample tilt angles (a).ϕ=22 , (b).ϕ=37 and (c).ϕ=52 . The curves in each panel represent different sample currents (SC) under a given beamline resolution (dE). For any given curve the sample current is nearly a constant.

FIG. 8: Energy shift as a function of sample current at different analyzer angles for the sample tilt angle of (a).ϕ=22 degrees and (b).ϕ=37 degrees. The spot size for these two cases is approximately 0.4mm×0.4mm. Note that while for the small analyzer angle the energy shift changes nearly linearly over the entire sample current range, for large analyzer angle, it shows a back bend at low sample current. If we take the value near zero sample current as the intrinsic Fermi level, it is found that the energy shift at high analyzer angle can be negative. (c). Energy shift per sample current for two different sample tilts angles. The slope is obtained by fitting the straight high sample current part as in Fig 8.

FIG. 9: Large energy-range valence band of Au measured at different analyzer angle α. The sample tilt angle is ϕ=37 degrees. In the inset shows the integrated spectral weight over the entire energy range of 5∼35 eV as a function of the analyzer angle α (black solid square). For comparison, the Fermi level as a function of the analyzer angle measured under similar condition is also plotted (blue circle).

FIG. 10: Numerical calculations of space charge effect. The pulse length is 60 ps and the spot size is 0.43mm×0.42mm. (a). The energy shift as a function of the number of interaction electrons from the space charge effect. The test electron has an energy of 30eV. Each curve represents the energy shift from the interaction electrons with an energy range of 0∼5 eV, 5∼10 eV, 10∼15 eV, 15∼20 eV, 20∼25 eV and 25∼30eV. (b). The corresponding energy broadening from the space charge effect for those six different energy regions. The inset of (a) illustrates the space charge effect that shows a number of electrons (solid circles) in a pulse escaping from the sample surface.

FIG. 11: The energy shift as a function of the interaction electron energy distribution for the space charge only, the mirror charge only, and both the space charge and the mirror charge. These values are obtained by extracting the slope of curves in Fig. 10a and 12a.

FIG. 12: Numerical calculations of combined space and mirror charge effect. The pulse length is 60 ps and the spot size is 0.43mm×0.42mm. (a). The energy shift as a function of the number of the interaction electrons from both space charge and mirror charge effects. The test electron has an energy of 30eV. Each curve represents the energy shift from the interaction electrons with an energy range of 0∼5 eV, 5∼10 eV, 10∼15 eV, 15∼20 eV, 20∼25 eV and 25∼30eV. (b). The corresponding energy broadening from both space charge and mirror charge for those six different energy regions. The inset of (a) schematically shows the mirror charge effect: a pulse of electrons (solid circles) escaping from the sample surface and each electron has a mirror charge (open circles) inside the sample.

FIG. 13: Time evolution of the energy shift. The data are obtained by averaging for 9, 30, 90 and 300 electrons/pulse.

FIG. 14: (a)Energy shift and (b)broadening per electron current (the unit is electrons per picosecond (e/ps))as a function of pulse length at different electron currents. The spot size is 0.43mm×0.42mm. For the energy shift, all curves overlap with each other, indicating that the energy shift is proportional to the electron current. But for the energy broadening, they do not strictly overlap with each other, particularly at longer pulse length.

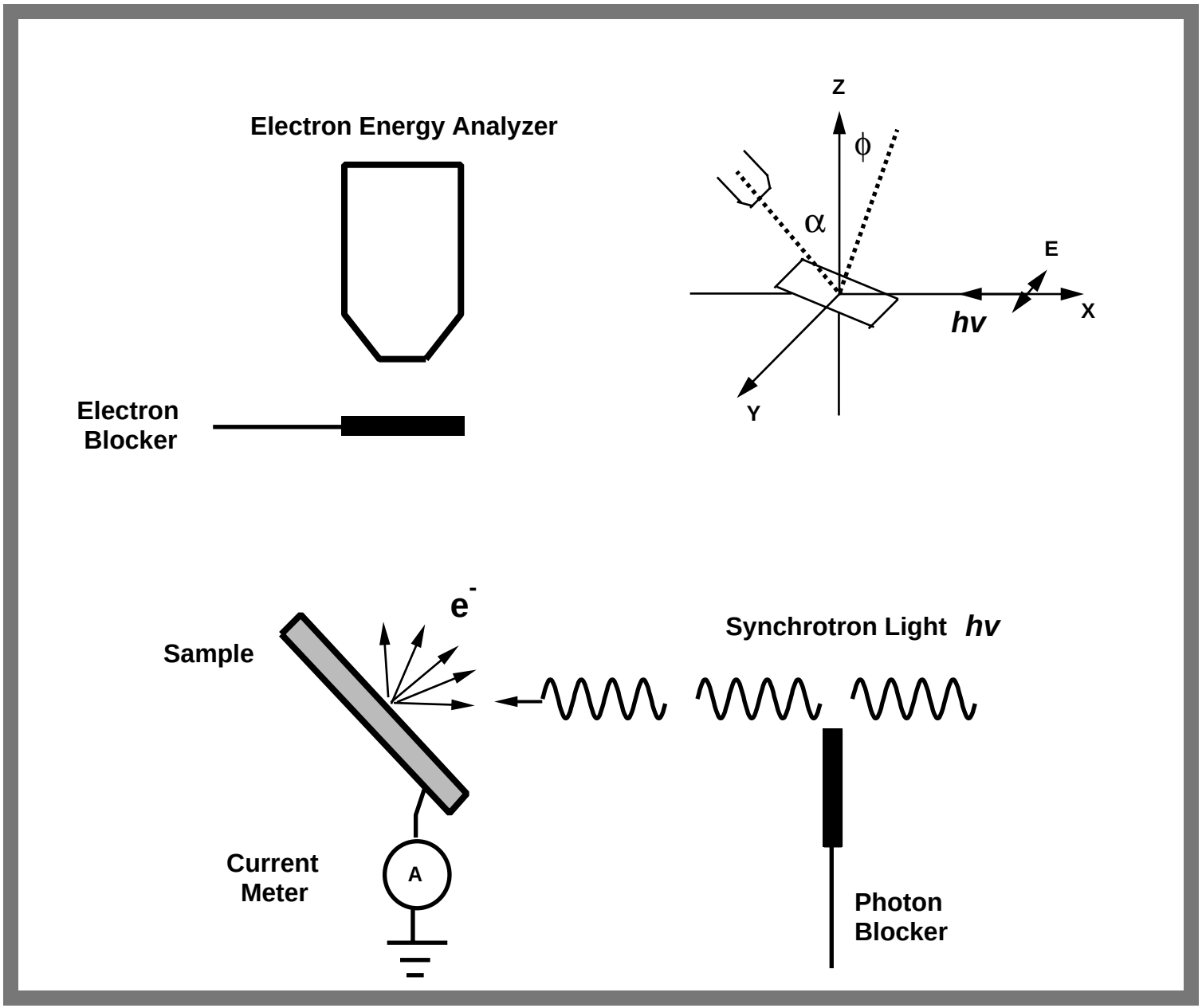

X. J. Zhou et al., Fig. 1

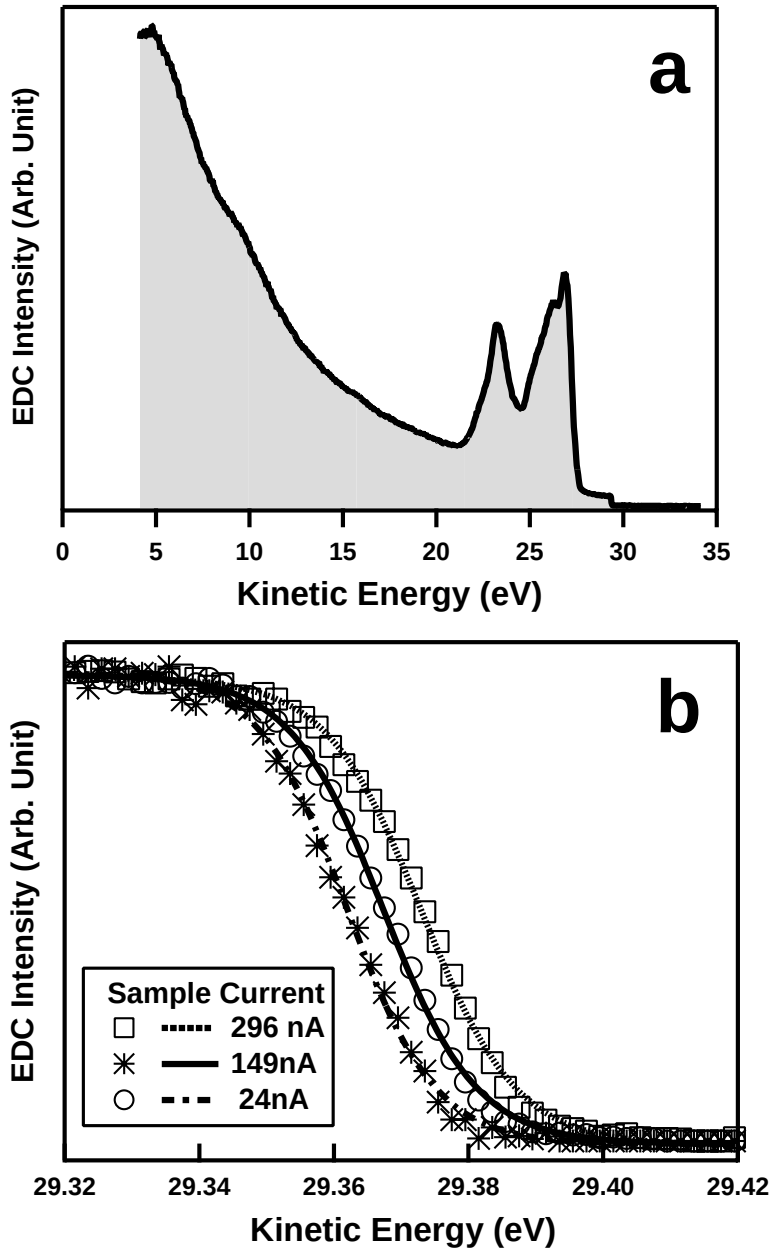

X. J. Zhou et al., Fig. 2

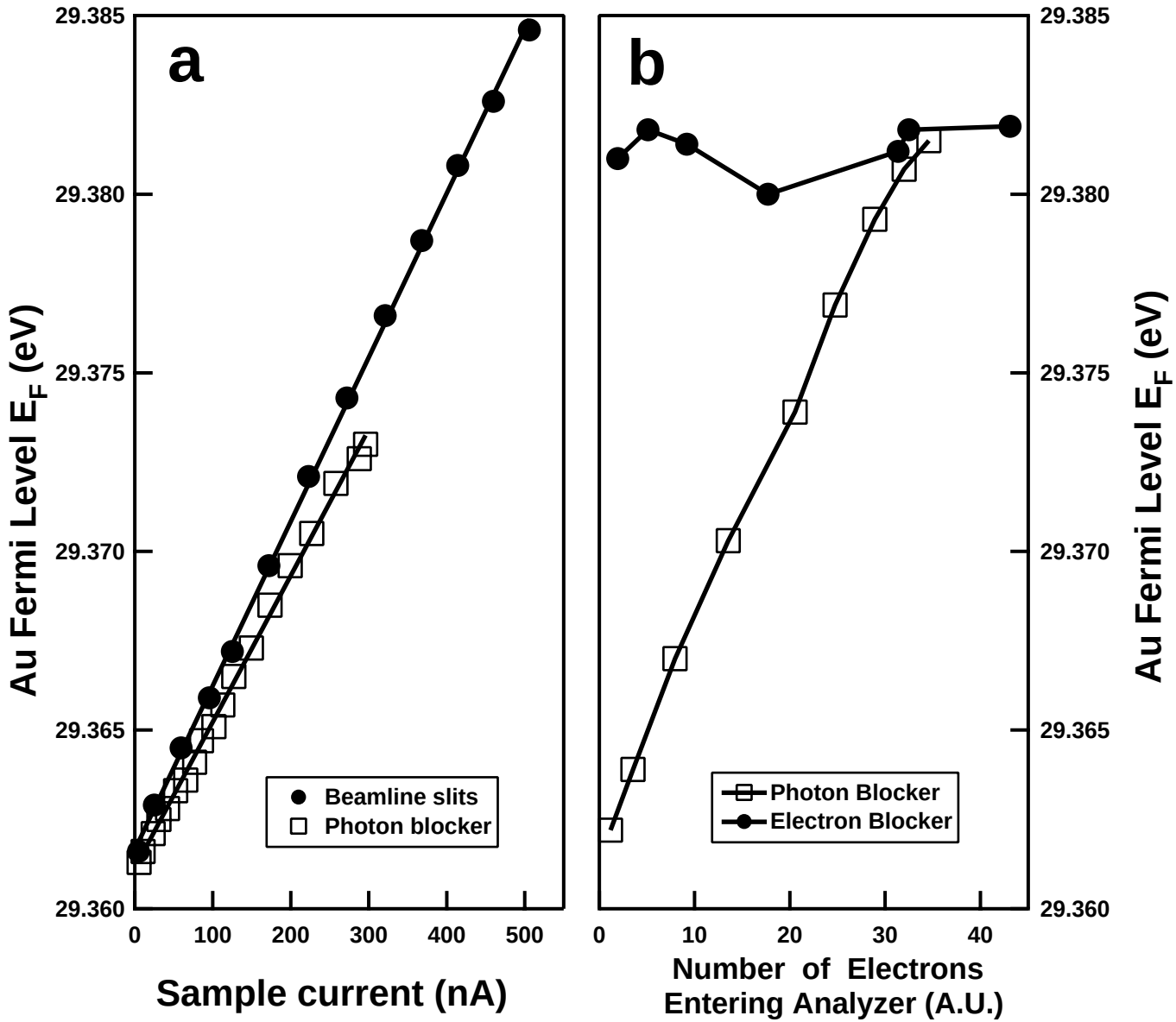

X. J. Zhou et al., Fig. 3

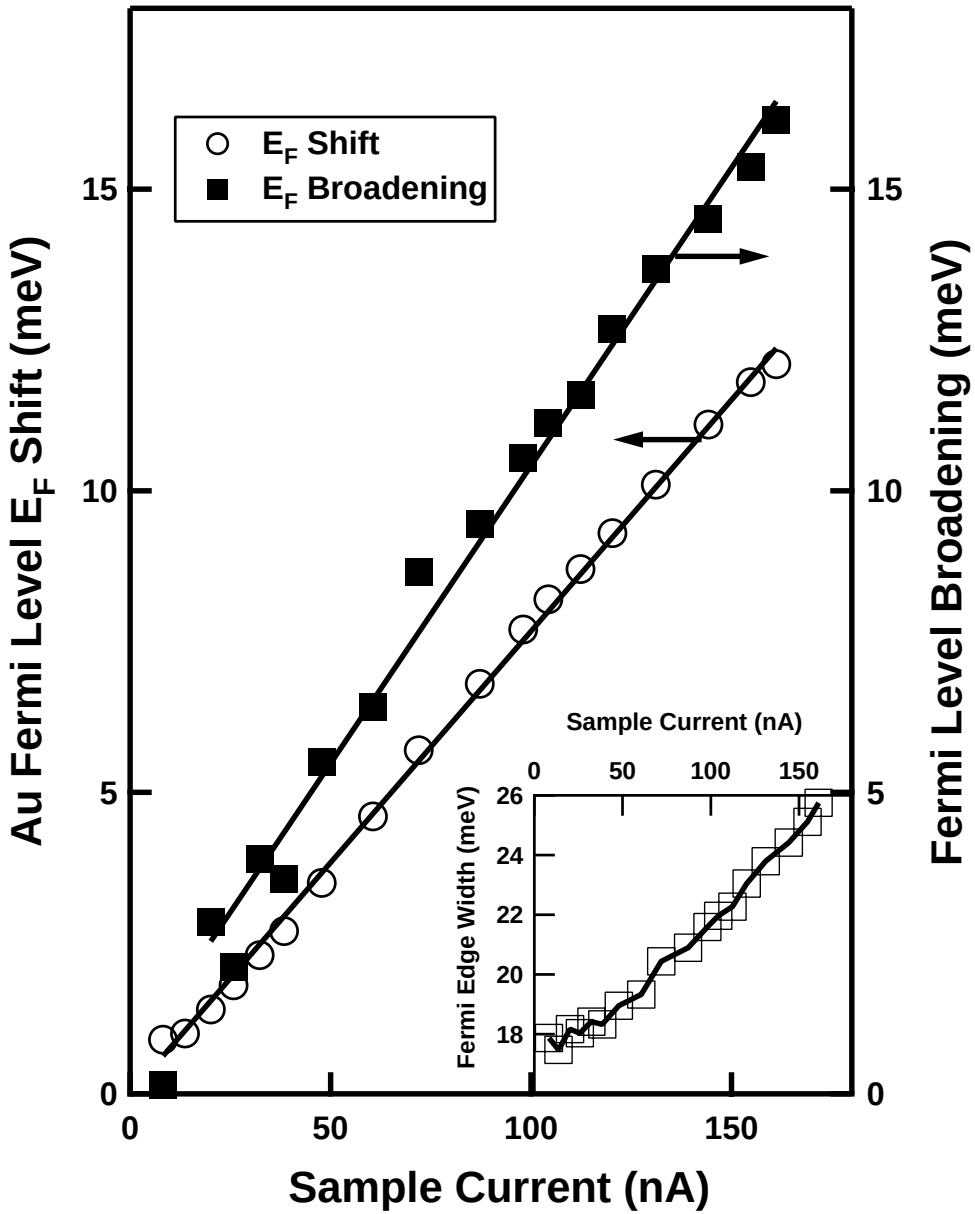

X. J. Zhou et al., Fig. 4

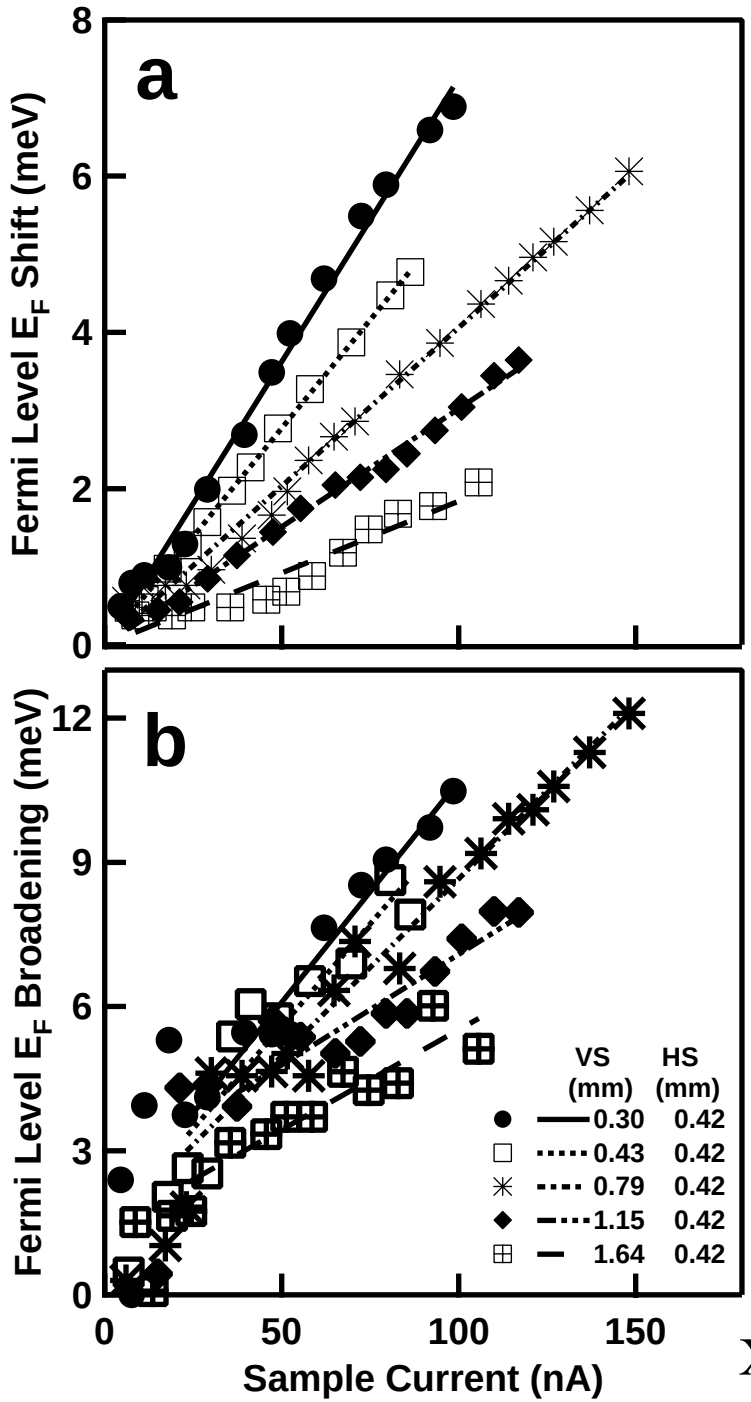

X. J. Zhou et al., Fig. 5

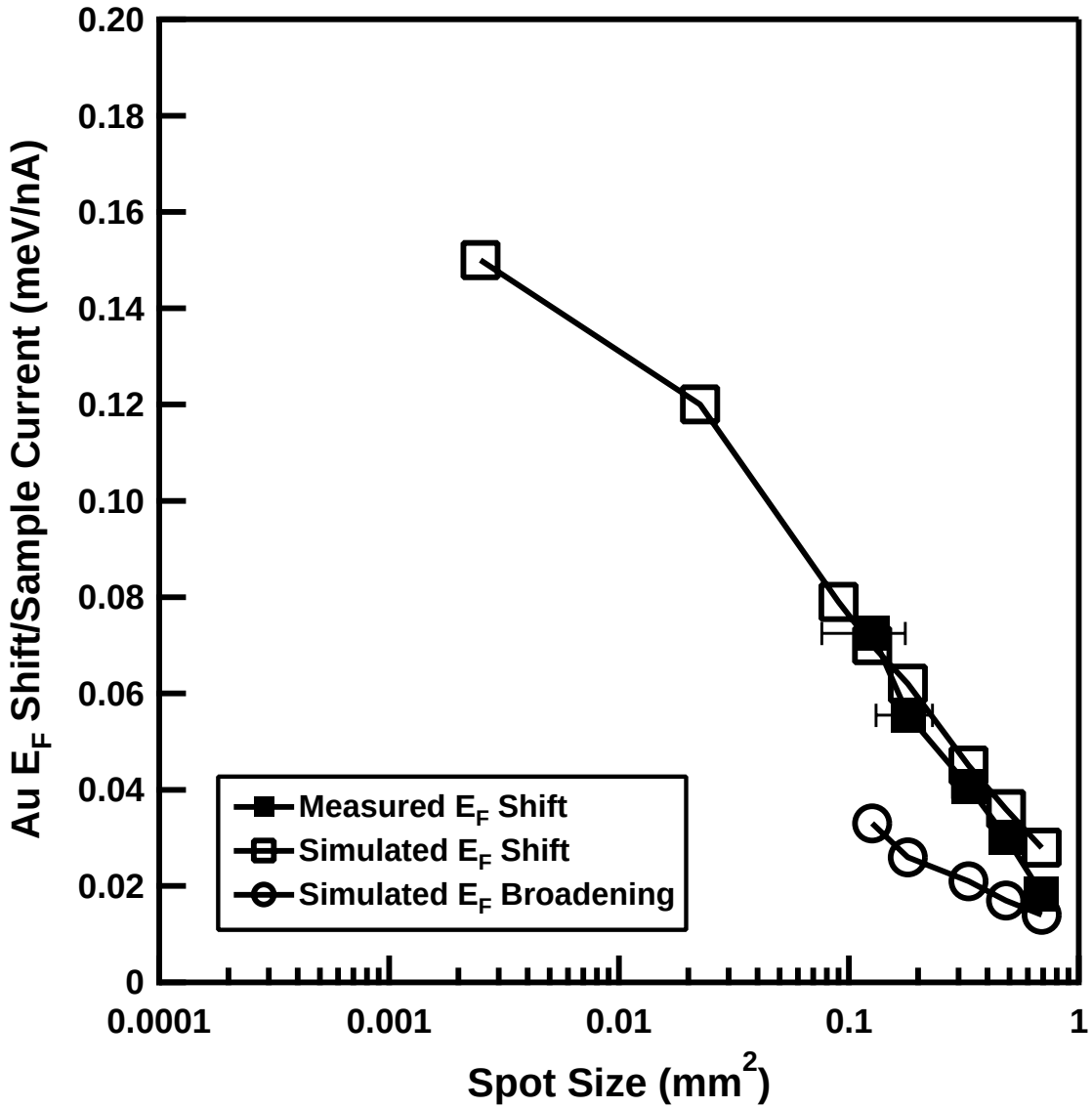

X. J. Zhou et al., Fig. 6

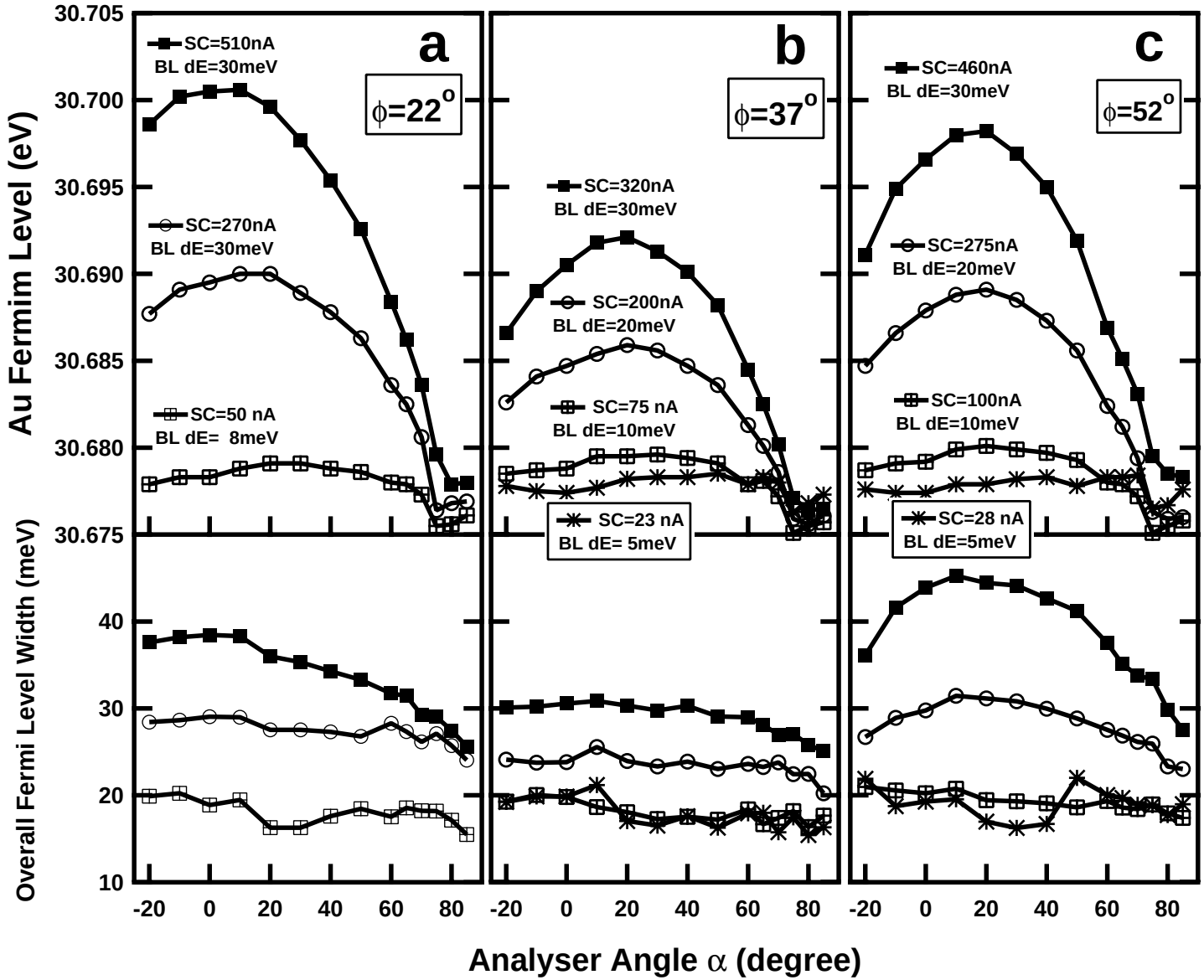

X. J. Zhou et al., Fig. 7

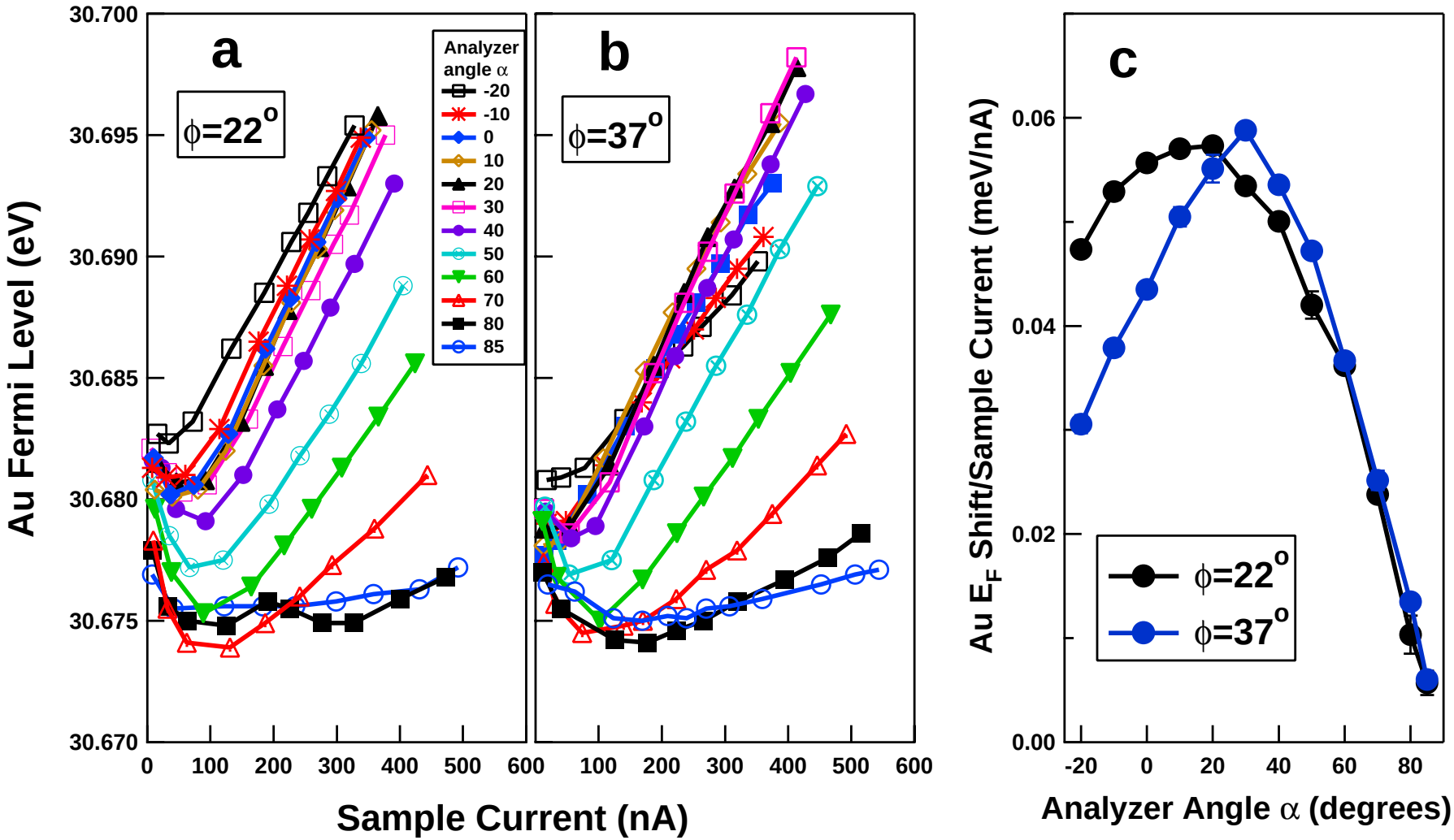

X. J. Zhou et al., Fig. 8

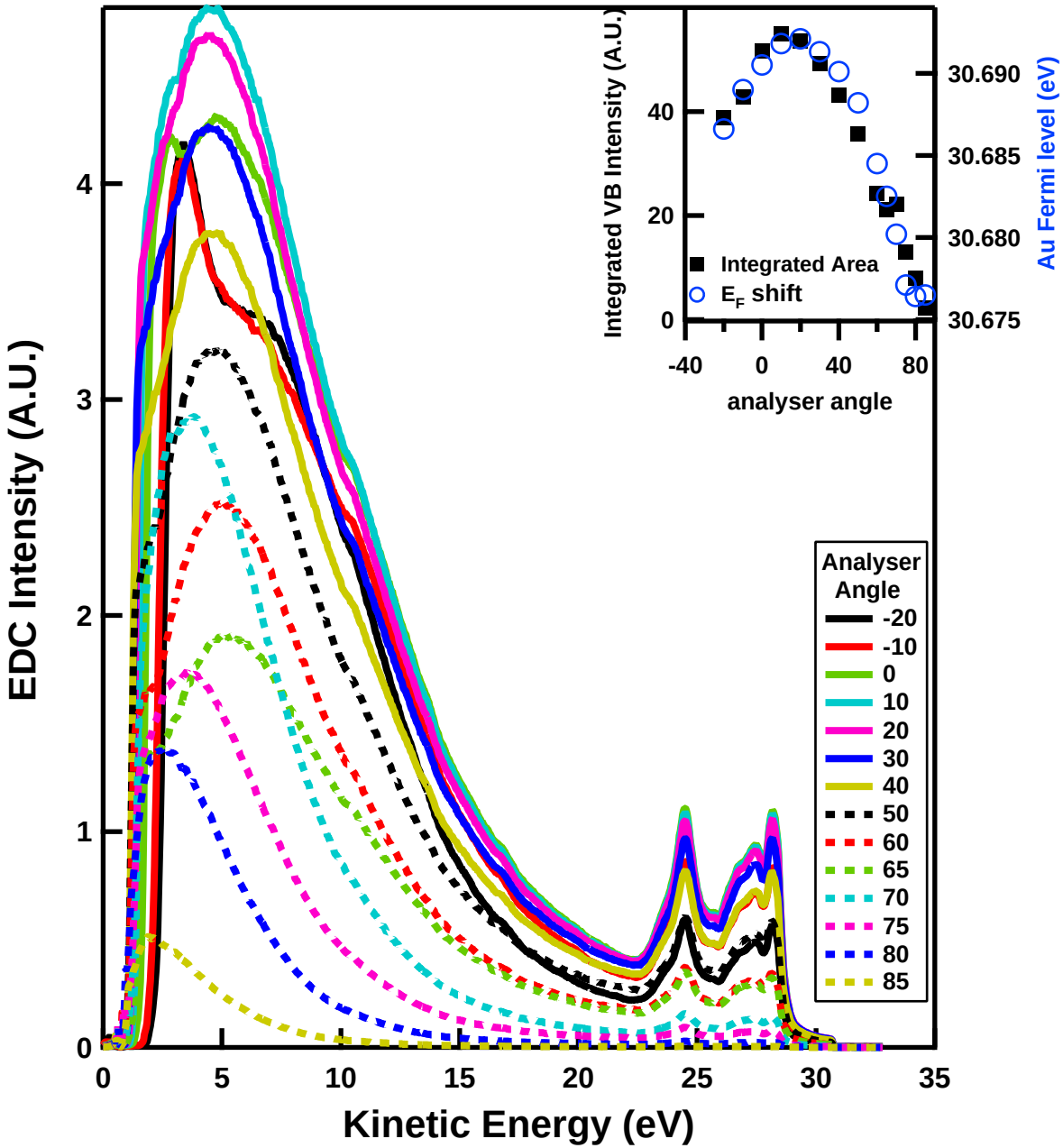

X. J. Zhou et al., Fig. 9

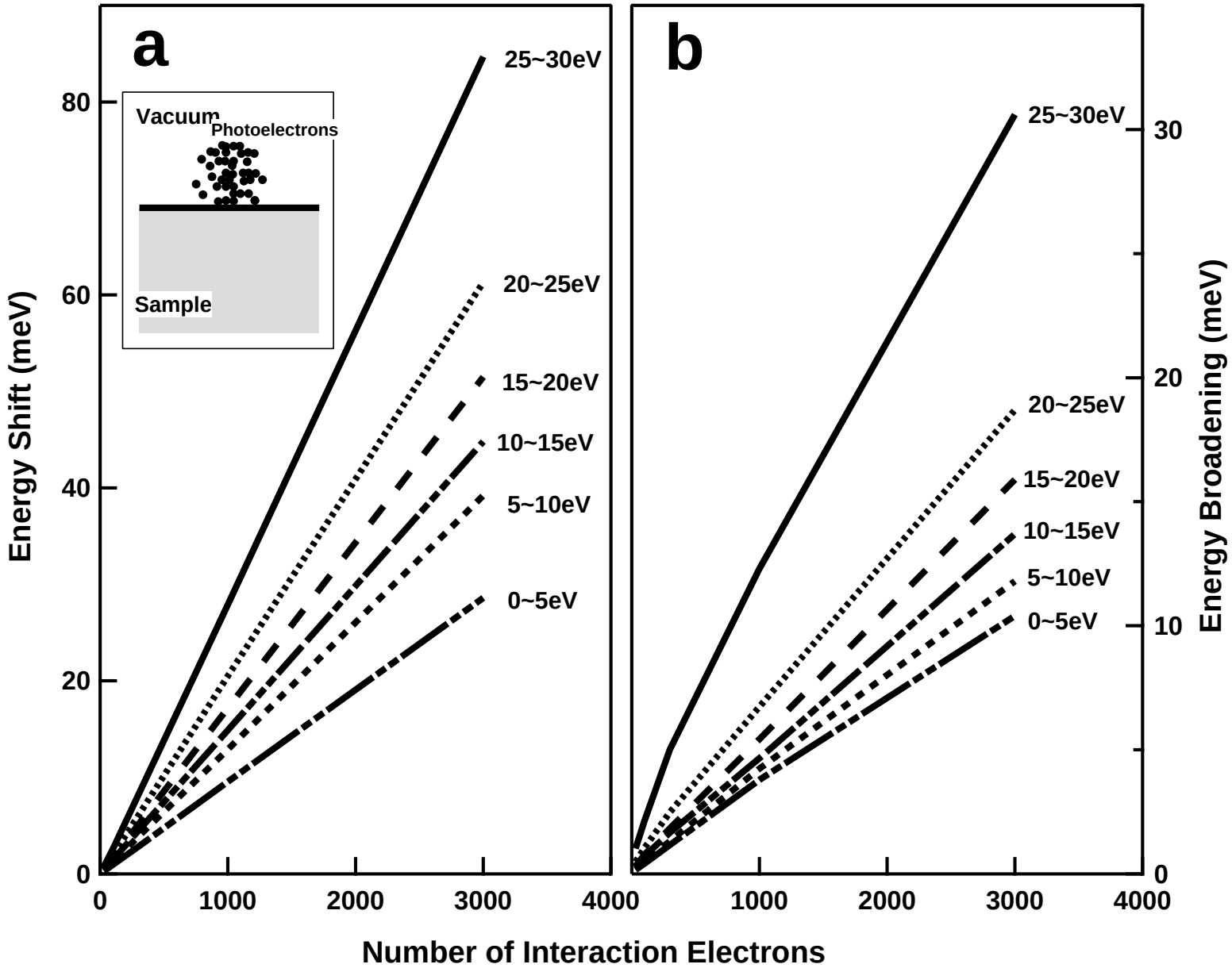

X. J. Zhou et al., Fig. 10

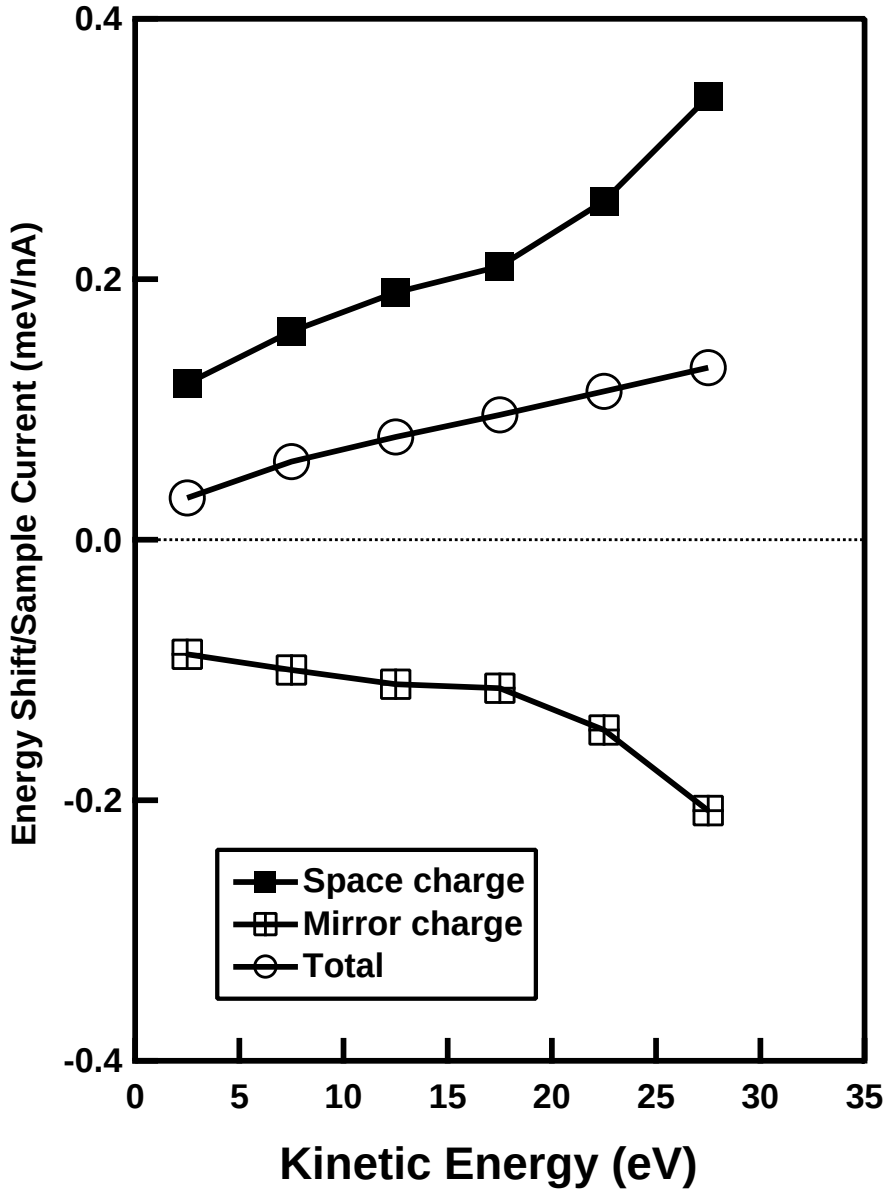

X. J. Zhou et al., Fig. 11

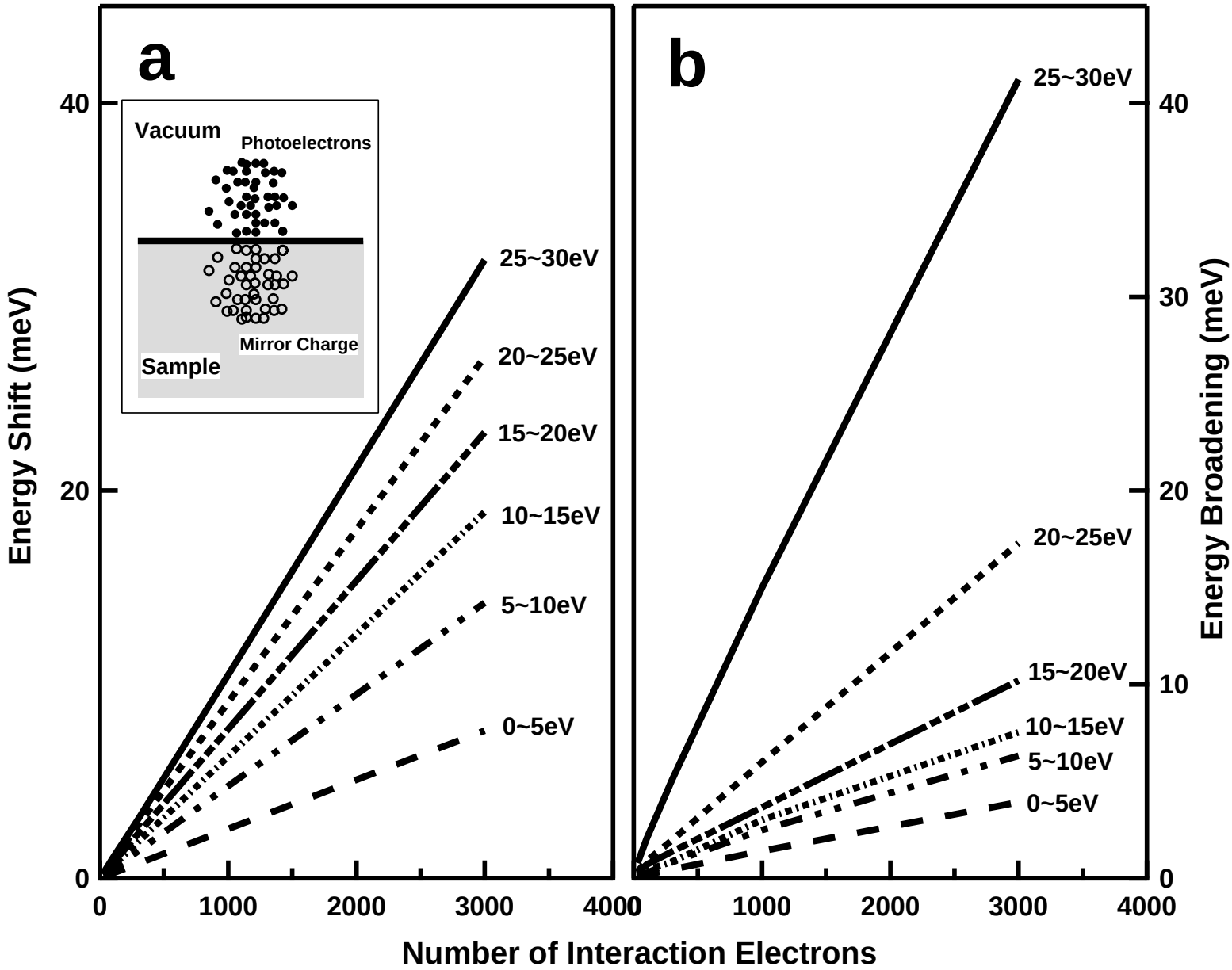

X. J. Zhou et al., Fig. 12

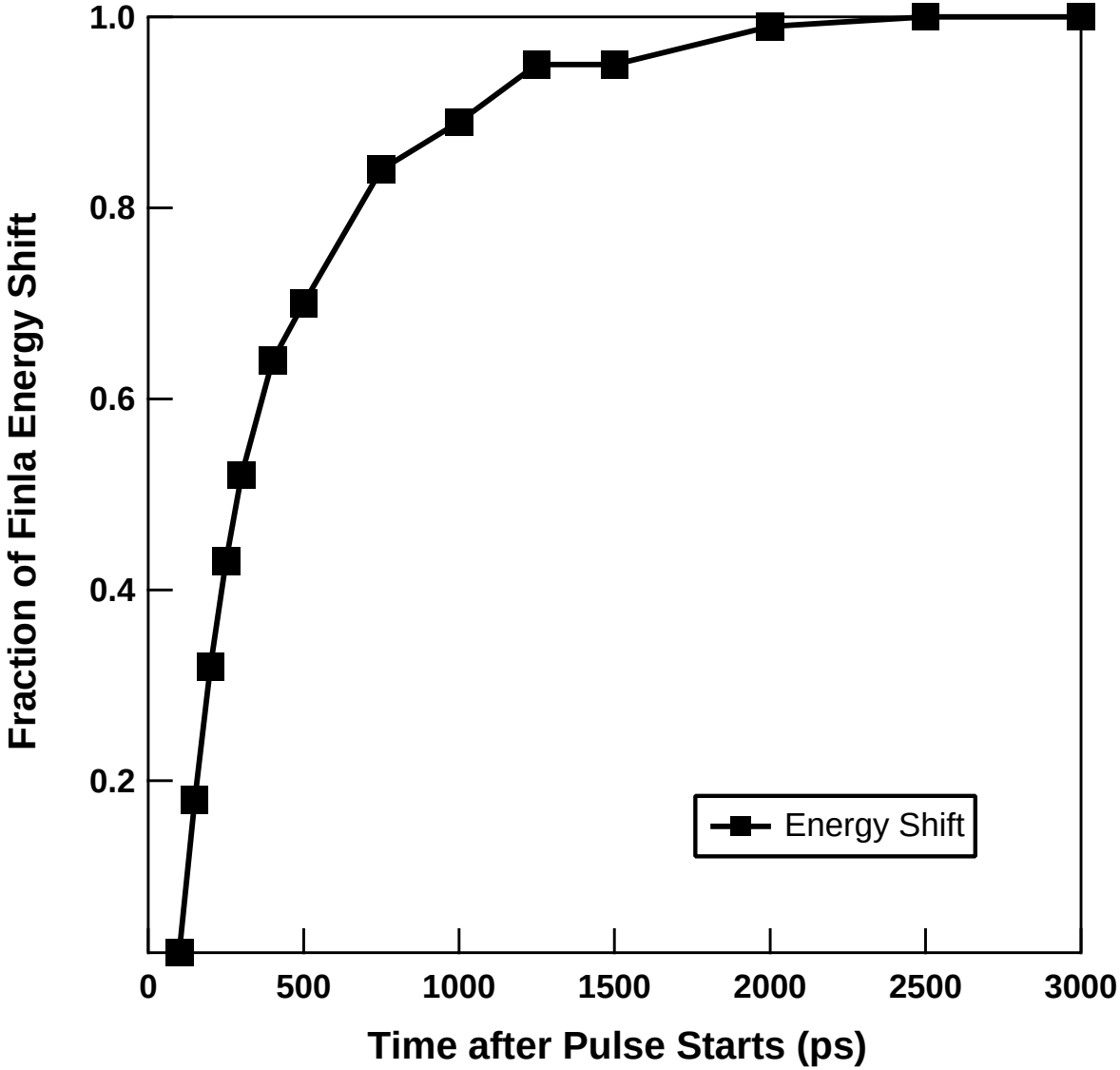

X. J. Zhou et al., Fig. 13

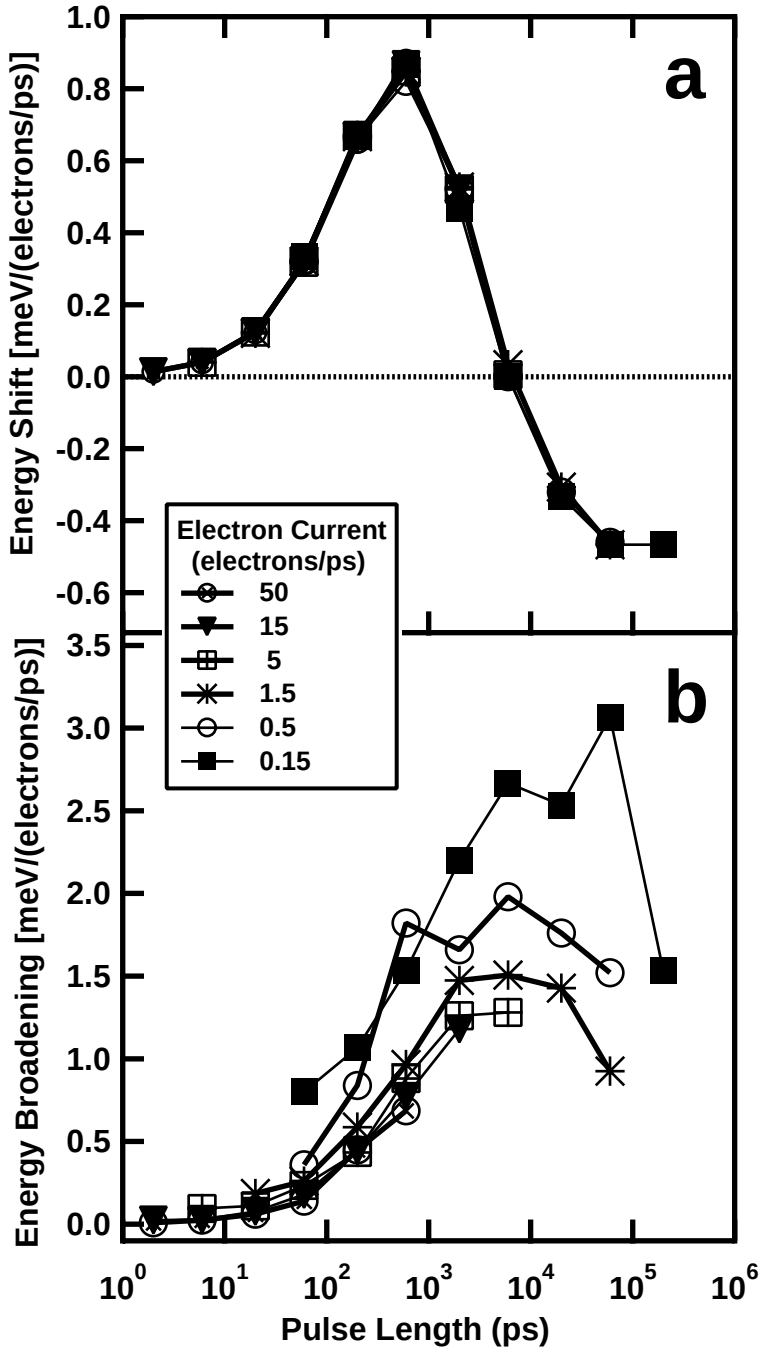

X. J. Zhou et al., Fig. 14